One-photon mass-analyzed threshold ionization spectroscopy of 1- and 2-iodopropanes in vacuum ultraviolet

Sang Tae Park, Sang Kyu Kim,[a] and Myung Soo Kim[b]
National Creative Research Initiative for Control of Reaction Dynamics and School of Chemistry, Seoul National University, Seoul 151-742, Korea

(Received 5 January 2001; accepted 16 January 2001)

One-photon mass-analyzed threshold ionization (MATI) spectroscopy of 1- and 2-iodopropanes has been studied using coherent vacuum ultraviolet (VUV) radiation generated by four-wave mixing in Kr gas. Accurate ionization energies to the lower and upper spin–orbit states of the molecular ions have been determined. These are 9.1755 ± 0.0005 and 9.6903 ± 0.0017 eV for the lower and upper spin–orbit states, respectively, of 2-iodopropane ion. For 1-iodopropane ion, *gauche* and *trans* peaks were resolved in the MATI spectra. Ionization energies to the lower spin–orbit states are 9.2567 ± 0.0005 and 9.2718 ± 0.0005, respectively, for the *gauche* and *trans* conformers. The corresponding values are 9.8332 ± 0.0017 and 9.8466 ± 0.0017 for the upper spin–orbit states. The pure ion beam of the *gauche*-only or that of *trans*-only could be selectively generated by tuning the VUV wavelength. Dissociation of 1- and 2-iodopropane ions, $C_3H_7I^+ \rightarrow C_3H_7^+ + I$, occurring in the ion core of highly excited Rydberg neutrals has been observed. Fragmentation thresholds for these reactions have been determined. This has led to an accurate potential energy diagram for the dissociation of the $C_3H_7I^+$ system in the threshold region. The heat of formation at 0 K of 2-$C_3H_7^+$ has been determined, 821.7 ± 3.8 kJ mol^{-1}, together with the proton affinity at 0 K of C_3H_6, 741.6 ± 3.9 kJ mol^{-1}. Plausible mechanisms for the production of 2-$C_3H_7^+ + I$ from 1-$C_3H_7I^+$ have been proposed. © *2001 American Institute of Physics.* [DOI: 10.1063/1.1353548]

I. INTRODUCTION

Zero electron kinetic energy (ZEKE) spectroscopy[1–4] is a powerful technique for high resolution spectroscopy of molecular ions. Multiphoton excitation is widely adopted in ZEKE spectroscopy to produce molecules in high Rydberg states. However, it is often difficult to obtain high quality multiphoton ZEKE spectra when molecules do not possess appropriate intermediate states. Single-photon excitation to the high Rydberg states using vacuum ultraviolet (VUV) light, or VUV ZEKE,[5] can be advantageous in this respect. The fact that various complications arising from the multiphoton effect with the use of high power lasers can be avoided is an additional advantage of the VUV ZEKE technique. A technique closely related to ZEKE is the mass-analyzed threshold ionization (MATI) spectroscopy,[6,7] which detects ions produced by pulsed-field ionization (PFI) of Rydberg molecules instead of the electrons as detected in ZEKE. Even though the two techniques are essentially identical in terms of the spectroscopic information they provide, ZEKE has been much more popular because the technique is more advanced such that spectra with higher quality can be obtained. However, the ability of MATI to identify the species responsible for the electrons ejected, and to produce state-selected molecular ions also, are important advantages in the spectroscopic and dynamical studies.[7]

Energetics of alkyl halide ions and their fragmentation near the reaction threshold have been of great research interest over the years.[8–11] The main reason for such research activities has been the importance of the thermodynamic data such as heats of formation of alkyl ions and proton affinities of hydrocarbons and utility of alkyl halide ions in their determination. Rosenstock and co-workers[9] reported the ionization energies to two ground spin–orbit states of some alkyl halide ions including the title ions and the appearance energies of fragments measured by the photoelectron–photoion coincidence (PEPICO) technique. With the experimental energy resolution of ~26 meV, the fragmentation onsets for both 1- and 2-iodopropane ions were found to lie close to or just above the upper spin–orbit states. Also found was that the heat of formation of $C_3H_7^+$ formed from 1-$C_3H_7I^+$ was nearly the same as that formed from 2-$C_3H_7I^+$ when correction was made for the reverse barrier using the kinetic energy release information available from metastable ion decomposition study. Hence, it was suggested that the fragmentation of 1-$C_3H_7I^+$ occur via isomerization to 2-$C_3H_7I^+$. Baer and co-workers[10] adopted a similar technique to study the kinetic energy release in the dissociation of iodopropane ions. It was suggested that the dissociation onset for 1-iodopropane ion corresponds to the upper spin–orbit state because the isomerization may take place only via the upper spin–orbit state. Recently, Baer and co-workers[11] remeasured the appearance energies of 2-$C_3H_7^+$ from 2-halopropanes using the PFI-PEPICO technique. This recent, and supposedly more accurate, result suggests that the fragmentation onset for 2-$C_3H_7I^+$ be noticeably higher than the ground vibrational level of the upper spin–orbit state.

[a]Permanent address: Department of Chemistry, Inha University, Inchon 402-751, Korea.
[b]Author to whom correspondence should be addressed.

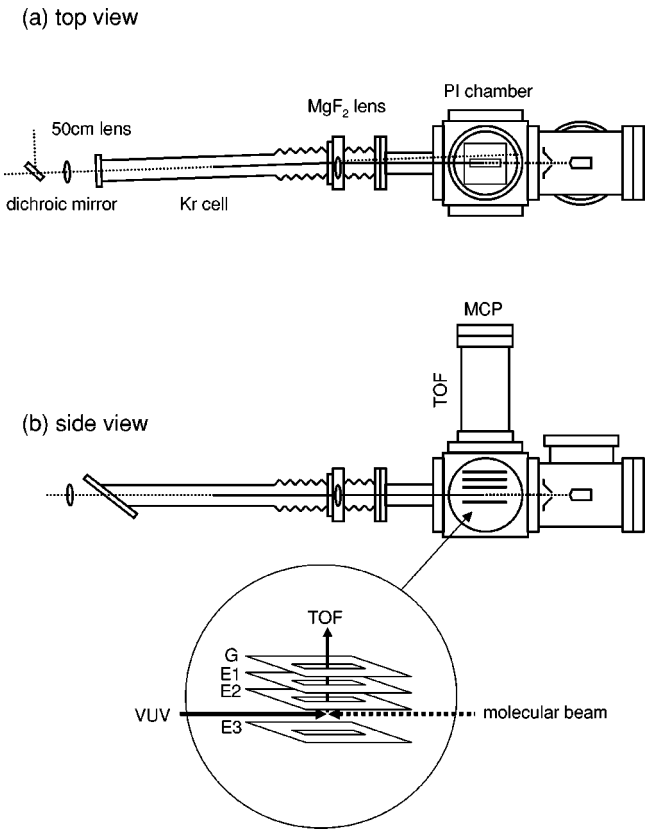

FIG. 1. Schematic drawing of the four-wave mixing cell and VUV MATI instrument. (a) top and (b) side views.

In this paper, we report the MATI spectra of 1- and 2-iodopropanes obtained by single-photon VUV excitation. Available from the spectra are the accurate spectroscopic and thermodynamic data for 1- and 2-iodopropane ions and their fragmentation thresholds. Observation of the dissociation occurring in the ion core of the high Rydberg states of 1-iodopropane is also reported.

II. EXPERIMENT

Iodopropanes were purchased from Aldrich and used without further purification. Samples were kept at room temperature, seeded in He or Ar carrier gas, expanded into a source chamber through a nozzle orifice (0.3 mm diam, General Valve), and skimmed through a 1 mm diam skimmer to enter a differentially-pumped ionization chamber. The backing pressure was ~1.5 atm typically and background pressure of the ionization chamber was maintained at 10^{-8} Torr.

The VUV laser pulse was generated by resonant four-wave mixing[12,13] in a Kr gas cell, Fig. 1. The UV laser pulse at 212.4 nm (0.3–1.0 mJ/pulse) was generated by frequency-doubling of the 425 nm output of a dye laser (Lambda-Physik, Scanmate II) pumped by the 355 nm output of an Nd:YAG laser (Continuum Surelite II, 5 ns duration), which was used to excite the Kr $5p[1/2]_0-4p^6$ transition via two-photon resonant absorption. Another laser pulse (5–50 mJ/pulse) in the 500–700 nm range generated by the second dye and Nd:YAG laser set was temporally and spatially overlapped with the above UV laser pulse in the Kr gas cell (5 Torr) to produce the VUV laser pulse in the wavelength range of 125–135 nm. Technically, two laser pulses were combined by using a dichroic mirror and loosely focused by a 50 cm focal-length fused-silica lens before entering the Kr gas cell. A MgF_2 lens (20 cm nominal focal length) was installed off-center at the exit of the Kr gas cell[14] such that the laser pulses passed through the edge of the lens. Because of the wavelength-dependence of the focal length, the VUV laser pulse could be spatially separated from the input laser pulses (UV and VIS) in the laser-molecular beam interaction region in the ionization chamber. The VUV output had an intensity of $\sim 10^{10}$ photons/pulse with a spectral resolution of 1 cm^{-1} and had the spot diameter of ~1 mm at the focus.

The VUV laser pulse was collinearly overlapped with the molecular beam in a counterpropagation manner[15] to maximize the laser-molecular beam interaction volume. Instead of the usual circular aperture, 4 mm×50 mm size slit-electrode assemblies were used to enhance ion collection efficiency, Fig. 1. The spoil field of 0.15–3.0 V/cm was applied in the ionization region to remove directly produced ions. To achieve pulsed-field ionization (PFI) of neutrals in the ZEKE state, an electric field of 5–135 V/cm was applied with the field direction perpendicular to that of the molecular and laser beams. Then, ions were accelerated, flied through a field-free region, and were detected by a dual microchannel plate (MCP) detector. It is well known that the spoil field must be kept low to obtain a MATI spectrum with good resolution,[16] which requires use of a long time delay between VUV absorption and PFI. Use of a time delay longer than 10 ns led to rapid decay of MATI signal in our apparatus. We could lengthen the lifetime of the VUV-excited neutrals tremendously, however, by applying a short pulse of scrambling field at the laser irradiation time.[17] This allowed the use of a very long delay time, ~40 μs, and low spoil field. Timing sequence for various pulses is shown in Fig. 2. The MATI signal detected by MCP was preamplified and A/D converted by a digital storage oscilloscope (LeCroy, LC334AM). Either the full time-of-flight mass spectrum or selected regions of the spectrum as needed were transferred to a personal computer in real time.

A double focusing mass spectrometer with reversed geometry (VG Analytical model ZAB-E) (Ref. 18) was used to record unimolecular dissociation, or metastable ion decomposition, of iodopropane ions. Samples were introduced into the ion source via a septum inlet and ionized by 70 eV electron ionization. Molecular ions generated in the ion source at 180 °C were accelerated to 8 keV and mass-separated by the magnetic sector. Product ions generated by unimolecular dissociation of the molecular ions were analyzed with the electric sector.

III. RESULTS AND DISCUSSION

Basic information available from ZEKE or MATI spectroscopy is the ionization energy of the neutral and the vibrational frequencies of molecular ions. Accurate determination of the former is known to be difficult due to the use of the PFI field.[16] Namely, a high PFI field ionizes Rydberg molecules with energy well below the ionization energy. Before measuring the ionization energies of 1- and 2-iodopropanes, we obtained the MATI spectrum of iodoet-

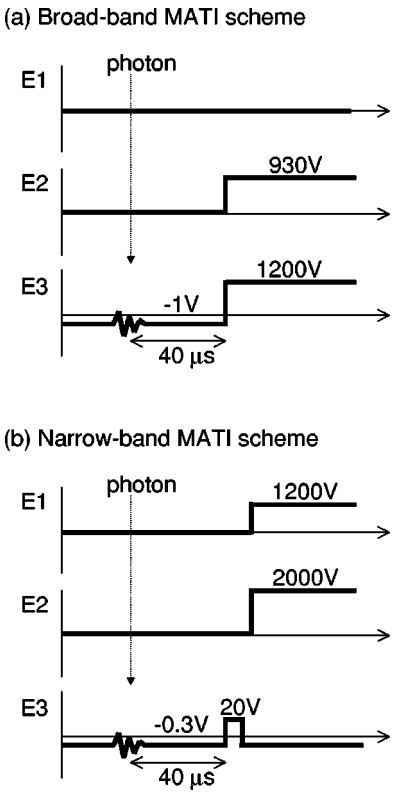

FIG. 2. Electrode voltage pulsing schemes. See Fig. 1 for the designation of electrodes. Two schemes are shown, (a) broad-band and (b) narrow-band MATI schemes. 1 V pulse is applied on E3 at the time of laser irradiation as the scrambling field and 40 μs delay between VUV and PFI pulses is used in both schemes. In the broad-band scheme, 1 V dc is applied on E3 to produce the spoil field of 0.5 V/cm until the PFI pulse. Simultaneous application of 1200 and 930 V on E3 and E2 electrodes, respectively, achieves field ionization and acceleration. In the narrow-band scheme, spoil and PFI fields are decreased to 0.3 V/2 cm and 20 V/2 cm, respectively. Ions generated and accelerated into the region between E2 and E1 by the PFI pulse are further accelerated by 2000 V on E2.

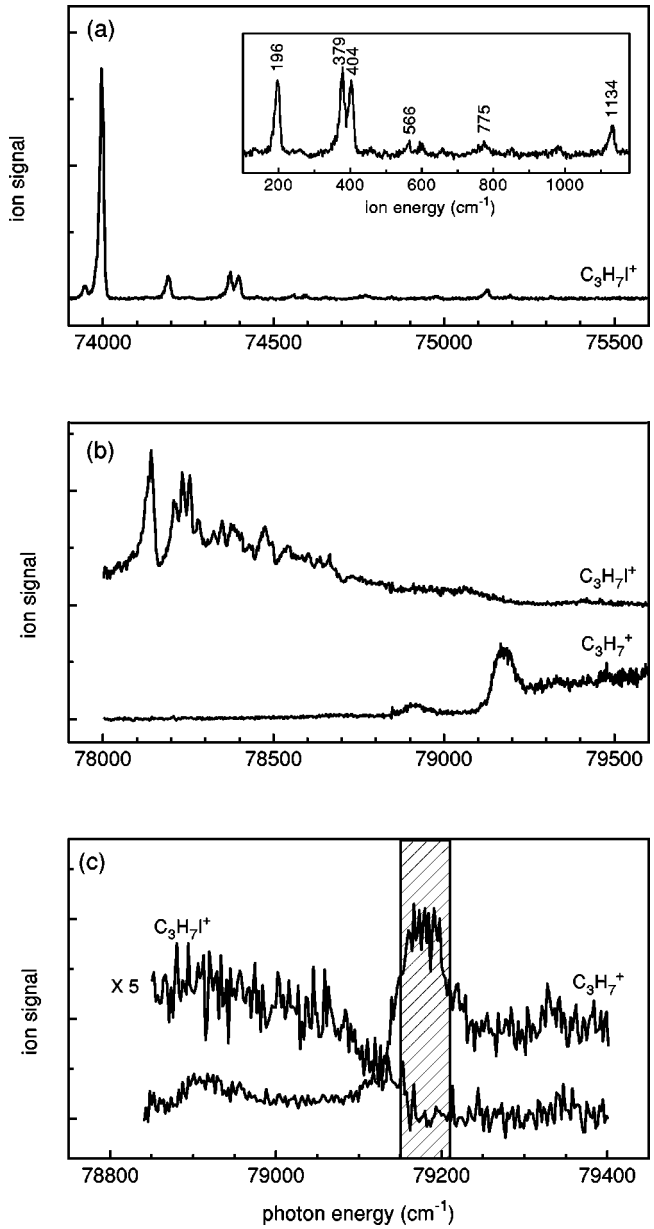

FIG. 3. One-photon VUV MATI spectra of 2-iodopropane. (a) $C_3H_7I^+$ generated in the lower spin–orbit state, (b) $C_3H_7I^+$ generated in the upper spin–orbit state and $C_3H_7^+$ produced therefrom. Fragmentation threshold region in (b) is magnified in (c) to show the appearance energy determination.

hane and compared the ionization energy determined therefrom with the literature value. The ionization energy in the MATI spectrum was measured at several PFI and spoil fields and extrapolated to the zero field, via multiple regression. The ionization energy of iodoethane became $75\,404\pm4$ cm^{-1} after correction, which agrees with the ZEKE measurement by Bondybey and co-workers,[19] $75\,406\pm5$ cm^{-1}, within error limits. We used the same method to determine the ionization energies to the lower spin–orbit states of 1- and 2-iodopropane ions. In the case of the ionization energies to the upper spin–orbit states and appearance energies of the fragments, $C_3H_7^+$ and I, this method could not be used because of very low signal levels. Instead, we measured these energies, including the ionization energies to the lower spin–orbit states, using a relatively high PFI field needed to obtain MATI spectra with reasonable quality. Then, the energy calibration factor was obtained by comparing these energies for the lower spin–orbit states with the accurate values. This was used to estimate other ionization and appearance energies.

A. VUV MATI spectroscopy of 2-iodopropane

The VUV MATI spectrum of 2-iodopropane near the threshold for ionization to the lower spin–orbit state is shown in Fig. 3(a). The prominent peak at $\sim$74 000 cm^{-1} most likely corresponds to the origin of the lower spin–orbit state. The weak peak appearing at somewhat lower energy is probably due to the transition from an excited vibrational level(s) of the neutral because its intensity got weaker as the higher backing pressure was used. The ionization energy to the lower spin-orbit state determined from the position of the main peak was $74\,005\pm4$ cm^{-1} (9.1755 ± 0.0005 eV) after correction. This compares well with the ionization energy determined previously by photoelectron spectroscopy (PES) (Refs. 20, 21) and by threshold photoelectron spectroscopy (TPES),[9] which were 9.18 ± 0.01 and 9.19 ± 0.01 eV, respectively. For vibrational assignment of bands appearing above the threshold [see the inset in Fig. 3(a) for their positions

TABLE I. Ionization energies (IE) of alkyl halides and appearance energies (AE) of propyl ions, in eV.

	C_2H_5I	1-C_3H_7I	2-C_3H_7I	Ref.
IE (X_1)[a]	9.3490±0.0005	9.2567±0.0005(G) 9.2718±0.0005(T)	9.1755±0.0005	this work
	9.3492±0.0006			19
		9.25±0.01	9.19±0.01	9
	9.35±0.01	9.26±0.01	9.18±0.01	20
IE (X_2)[a]	9.9327±0.0017	9.8332±0.0017(G) 9.8466±0.0017(T)	9.6903±0.0017	this work
	9.9324±0.0006			19
		9.84±0.01	9.77±0.02	9
	9.93±0.01	9.82±0.01	9.75±0.01	20
AE($C_3H_7^+$)		9.8332±0.0017	9.8180±0.0037	this work
			9.851±0.025	11
		9.84±0.01	9.77±0.02	9
			9.82±0.01[b]	8

[a]X_1 and X_2 designate the lower and upper spin–orbit states, respectively, of the molecular ions.
[b]298 K onset reported by Traeger (Ref. 8) was converted to 0 K value by Baer and co-workers in Ref. 11.

relative to the origin], *ab initio* calculation was performed for 2-iodopropane ion at the MP2 level using the LanL2DZ basis set.[22] The calculated frequencies for the C–I bending and stretching vibrations were 192 and 387 cm^{-1}, respectively, at this level. Hence, the band at 196 cm^{-1} in the MATI spectrum is assigned to the C–I bending. In the C–I stretching region of the spectrum, two bands appear, namely, at 379 and 404 cm^{-1}. 2-Iodopropane ion in its ground state has a plane of symmetry connecting H–C–I atoms. The C–I bending and stretching vibrations are both in-plane modes, and thus belong to the same symmetry. Since the first overtone of the C–I bending and the fundamental of the C–I stretching are very close in energy, it is highly likely that the above doublet is due to Fermi resonance of these vibrations. The band at 565 cm^{-1} is due to the second overtone of the C–I bending ($196\times3=588$) and the band at 775 cm^{-1} is due to the first overtone of the C–I stretching mode. The relatively strong band at 1134 cm^{-1} is assigned tentatively to the C–C stretching mode. The fact that the vibrational bands in the MATI spectrum are mostly due to excitation of C–I modes is understandable because the transition to the Rydberg states probably involves an electron in the nonbonding orbital of the iodine atom. Also the fact that the origin band is much stronger than others means that the molecular geometry does not change much upon promotion of this electron.

The origin of the upper spin–orbit state of 2-iodopropane ion also appears as a sharp peak in the MATI spectrum, Fig. 3(b). The ionization energy to this state becomes 78 157±14 cm^{-1} (9.6903±0.0017 eV) after correction. This is somewhat smaller than 9.75±0.01 eV determined previously by PES.[20] The MATI spectrum just above the origin of the upper spin–orbit state displays complex structures with a broad background, which might have led to overestimation of the ionization energy in the previous low-resolution PES work. We could not assign the structures in this MATI spectrum to the vibrational modes in the upper spin–orbit state. It is likely that the complex structures in the spectrum arise because optically bright states in the upper spin–orbit state are strongly coupled with dark states in the lower spin–orbit state. The vibrational energy of the lower spin-orbit state corresponding to the upper spin–orbit state origin is ~4150 cm^{-1} (see Table I). The density of states in the lower spin–orbit state at this energy calculated with the *ab initio* vibrational frequencies is $4.8\times10^2/cm^{-1}$. Thus, the vibrational assignment for the structures in the upper state MATI spectrum would not be feasible with the resolution achieved in this work.

Also shown in Fig. 3(b) is the MATI spectrum obtained by recording the fragment ion, $C_3H_7^+$, signal. The fact that $C_3H_7^+$ was detected by PFI of one-photon excited Rydberg neutral means that dissociation occurred in the ion core of the Rydberg neutral and the Rydberg electron was retained in the C_3H_7 moiety, for as long as 40 μs of the time delay between the VUV laser and PFI pulses. Ion core dissociation has been reported for several systems including benzene,[4] Ar–benzene cluster,[23] and HBr.[24] In addition to the main band at ~79 180 cm^{-1}, a weak band appears at ~78 930 cm^{-1} in the fragment ion MATI spectrum. There is hardly any fragment ion signal between these two bands while the parent ion signal is present. This leads us to conclude that the weak band is due to vibrationally excited neutral and the fragmentation threshold lies close to the main band position. The fragmentation threshold was estimated by considering the frequency at which the parent ion signal disappears and the frequency at the main band position, Fig. 3(c), which is 79 188±29 cm^{-1} (9.8180±0.0037 eV) after correction. Baer and co-workers[11] converted the photoionization efficiency data reported by Traeger[8] and obtained the 0 K onset of 9.82±0.01 eV. This is in excellent agreement with the present result. On the other hand, the 0 K onset determined by Baer and co-workers[11] with PFI-PEPICO, 9.851±0.025 eV, is a little larger than the present result while the threshold PEPICO result obtained by Rosenstock and co-workers,[9] 9.77±0.02 eV, is a little smaller. Disagreement with the former is especially disturbing because the PFI-PEPICO experiment was done with very high photon resolution (<0.001 eV) and because their measurements for three

2-halopropanes (chloro, bromo, and iodo) led to similar heat of formation data for the 2-propyl ion. In the analysis of the breakdown diagrams obtained by PFI-PEPICO, Baer and co-workers assumed that all ions with energies in excess of the dissociation limit fragment within 1 μs. This assumption is in contradiction with the lifetime in the microsecond range near the threshold suggested by Rosenstock and co-workers.[9] The latter was based on the observation that the breakdown diagram shifted slightly as the source residence time was varied in the microsecond range and that metastable ion decomposition, $2\text{-}C_3H_7I^+ \rightarrow 2\text{-}C_3H_7^+ + I$, was observed with a double focusing mass spectrometer. In this work, we also recorded the metastable ion decomposition and could reproduce the result by the above investigators. Since the metastable ion decomposition occurred 15–30 μs after the molecular ion formation in our apparatus and its intensity was very weak, it is likely that the rate constant for dissociation of $2\text{-}C_3H_7I^+$ near the threshold is 10^5–$10^6\ s^{-1}$. We could observe similar metastable ion decomposition signals for other 2-halopropane ions also. The fact that the lifetime of $2\text{-}C_3H_7I^+$ is longer than 1 μs near the threshold suggests the possibility that the appearance energy was overestimated in the work of Baer and co-workers. We have confidence in the reliability of the present result because the single-photon MATI technique using VUV laser adopted here has better resolution than the PFI-PEPICO technique using the synchrotron radiation and because much longer time delay was used here than in PEPICO experiments. Ionization and appearance energies of 2-iodopropane system determined in this work are listed in Table I and drawn schematically in Fig. 5.

Accurate determination of these values allows further discussion on the energetics and dissociation of the system. Appearance energy of $2\text{-}C_3H_7^+ + I$, 9.8180±0.0037 eV, is a little higher than the onset of the upper spin–orbit state of $2\text{-}C_3H_7I^+$, 9.6903±0.0017 eV. Namely, additional internal energy above the onset of the upper spin-orbit state is needed for the dissociation of $2\text{-}C_3H_7I^+$. Also, strong coupling between the upper and lower spin–orbit states as manifested by complex structures in the MATI spectrum obtained by recording the molecular ion near the upper state ionization threshold suggests efficient conversion between these states. Then, the dissociation may occur in the lower spin–orbit state, possibly statistically. We also reevaluated the heat of formation of $2\text{-}C_3H_7^+$ and the proton affinity of C_3H_6 using the related thermochemical data in Table II. These values at 0 K were 821.7±3.8 and 741.6±3.9 kJ mol^{-1}, respectively. The latter agrees very well with 740.3 kJ mol^{-1} obtained by Smith and Radom through *ab initio* calculation at the G2 level.[25] The error limits in the above data are almost entirely due to that in the heat of formation of $2\text{-}C_3H_7I$ neutral available in the literature. More accurate results may become available with VUV MATI work on the $2\text{-}C_3H_7Cl$ system.

TABLE II. Thermochemical data at 0 K, in kJ mol^{-1}.

	0 K value	Method	Ref.
$\Delta_f H^0(2\text{-}C_3H_7I)$	−18.4±3.8		32
$\Delta_f H^0(I\ ^2P_{3/2})$	107.2		33
$\Delta_f H^0(H^+)$	1528.0		34
$\Delta_f H^0(C_3H_6)$	35.3±0.8		32
$AE(2\text{-}C_3H_7^+ + I)$[a]	947.29±0.35	MATI	this work
	950.5±2.4	PFI-PEPICO	11
	943±2	PEPICO	9
	947±1[b]	PIE	8
$\Delta_f H^0(2\text{-}C_3H_7^+)$	821.7±3.8	MATI	this work
	825.0±1.5	PFI-PEPICO	11
	817±4	PEPICO	9
	822±4	PIE	8
$PA(C_3H_6)$[c]	741.6±3.9	MATI	this work
	738.3±1.5	PFI-PEPICO	11
	746±4	PEPICO	9
	741±4	PIE	8
	742±4	proton-transfer rex.	35
	740.3	G2	25
	740.4	MP4/6-311G**	36

[a]Appearance energy from $2\text{-}C_3H_7I$.
[b]298 K value reported by Traeger (Ref. 8) was converted to 0 K value by Baer and co-workers in Ref. 11.
[c]Proton affinity.

B. VUV MATI spectroscopy of 1-iodopropane

Two conformers are present for 1-iodopropane, *gauche* and *trans*.[26–28] Since their energies are very similar, the gas phase molecule is known to exist as a mixture with the ratio *gauche:trans*=2:1 because two configurations are possible for the *gauche* form and one for the *trans*. It has been difficult to determine their relative stabilities. *Ab initio* calculation[28] at the HF/LANL1DZ level showed that the *trans* form was a little more stable while the molecular mechanics calculation[28] showed that the two forms had nearly the same energy. Hagen and co-workers[28] performed the gas phase electron diffraction study of 1-iodopropane and reported that the *gauche* form might be more stable, but only by 0.2±0.4 kcal mol^{-1} (0.8±1.7 kJ mol^{-1}). All these suggest that the *gauche* and *trans* forms of neutral 1-iodopropane are nearly the same in energy, which will be assumed in this work. On the other hand, the barrier heights for the *gauche–trans* transformation calculated by *ab initio* and molecular mechanics calculations are rather similar, ~14 kJ mol^{-1}.

Figure 4(a) shows the VUV MATI spectrum of 1-iodopropane near the ionization threshold to the lower spin–orbit state. Considering that two conformers exist for the neutral 1-iodopropane, and for the molecular ion also, and that the origin of the lower spin–orbit state appeared prominently for 2-iodopropane, two strong peaks at ~74 660 and ~74 780 cm^{-1} must be due to the generation of the conformeric ions in the ground state. The VUV transition involves promotion of an electron from the iodine nonbonding orbital and its transition dipole moment would not be much affected by the position of the terminal methyl group. Then, considering the *gauche:trans* ratio of 2:1 in the neutral and the intensity ratio in the VUV MATI spectrum, it is reasonable to assign the bands at ~74 660 and ~74 780 cm^{-1} to the *gauche* and *trans* forms, respectively. The ionization energies to the lower spin–orbit states of the *gauche* and *trans* forms become 74 660±4 cm^{-1} (9.2567±0.0005 eV) and 74 782±4 cm^{-1} (9.2718±0.0005 eV), respectively,

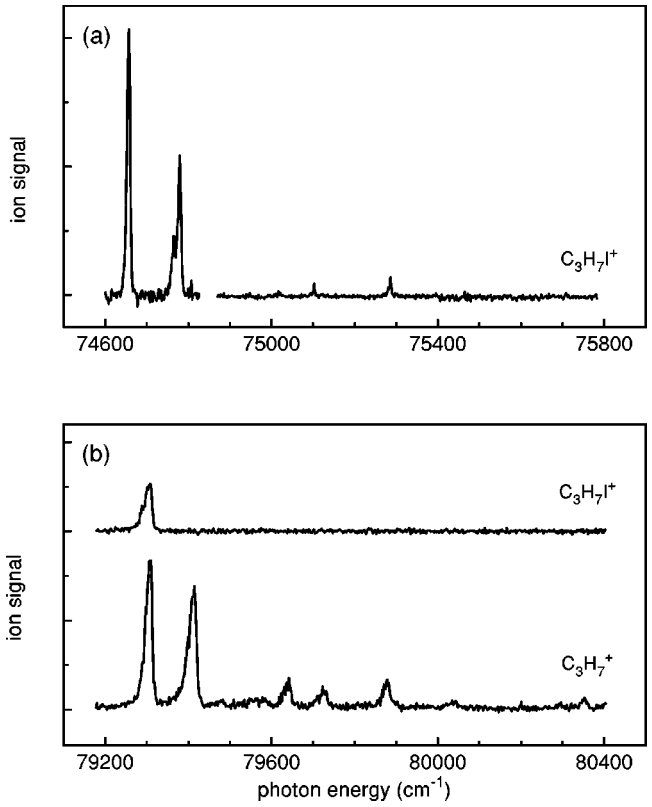

FIG. 4. One-photon VUV MATI spectra of 1-iodopropane. (a) $C_3H_7I^+$ generated in the lower spin–orbit state and (b) $C_3H_7I^+$ generated in the upper spin–orbit state and $C_3H_7^+$ produced therefrom.

after correction. The previous PES (Ref. 20) and threshold PEPICO (Ref. 9) studies, which could not resolve the conformer peaks, reported the ionization energies of 9.26 ± 0.01 and 9.25 ± 0.01 eV, respectively. Assuming that the *gauche* and *trans* conformers of the neutral 1-iodopropane have nearly the same energy, the difference of 122 cm^{-1} in ionization energies means that the *gauche* form is more stable by as much than the *trans* form for the ionic species. Proximity of the electron-donating CH_3 group to the iodine atom seems to stabilize the *gauche* form more than the *trans* form in the case of the positive ion. It is important to note that the sharp peaks at 74 660 and 74 782 cm^{-1} correspond to the *gauche* and *trans* ions, respectively, with hardly any internal energy. Assuming that the *gauche–trans* barrier for 1-iodopropane ion is similar to that for the neutral, ~14 kJ mol^{-1} (~1200 cm^{-1}), there will be no further interconversion between the conformeric ions generated at these wavelengths. Namely, an ion beam consisting of single conformer, either *gauche* or *trans*, has been generated by VUV MATI of 1-iodopropane. Selective generation of conformeric ion beams of 9-ethylfluorene with two color 1+1 MATI was reported by Pitts and co-workers,[29] where conformer selection was achieved spectroscopically in the $S_1 \leftarrow S_0$ transition step. The present method, which uses one-photon excitation to the Rydberg states near the ionization limit, does not require a bound intermediate state for conformer selection and may be more generally applicable. Generation of a pure conformeric beam will allow the study of conformation dependence of reaction dynamics. In the case of the 1-iodopropane neutral, the excited state dynamics of *gauche* and *trans* conformers on the repulsive electronic states has been reported.[30,27] Additional vibrational bands appear in the VUV MATI spectrum in Fig. 4(a). Assignment for these bands was difficult because presence of two conformers had to be taken into account and because *ab initio* calculation was not possible for 1-iodopropane ion.

Much more dramatic spectral features are observed in the VUV MATI spectra near the threshold region for the upper spin-orbit states of 1-iodopropane ions, Fig. 4(b). In the VUV MATI spectrum obtained by recording the parent ion signal, only one peak is observed near the threshold with significant intensity. One can neither understand why only one peak appears nor determine which of the two conformers are responsible for this peak from this spectrum alone. The answer can be found from the MATI spectrum obtained by recording the fragment ion signal drawn in the same figure. Two peaks appear prominently at ~79 300 and ~79 400 cm^{-1} in the fragment ion MATI spectrum. Separation between the two peaks is comparable to that between the two threshold peaks in the lower spin–orbit state spectrum. Hence, the former can be assigned to the *gauche* conformer and the latter to *trans*. Since the prominent peak in the parent ion MATI spectrum is located at the same frequency as the *gauche* band in the fragment ion spectrum, this can be assigned to the ionization onset to the upper spin–orbit state of the *gauche* conformer. Namely, the *gauche* conformer dissociates partially at the upper spin–orbit state onset and is detected both in the parent and fragment ion spectra while the *trans* form dissociates completely and is detected in the fragment ion spectrum only. Ionization energies to the upper spin–orbit states of the *gauche* and *trans* conformers are $79\,310\pm14$ cm^{-1} (9.8332 ± 0.0017 eV) and $79\,419\pm14$ cm^{-1} (9.8466 ± 0.0017 eV), respectively, after correction. The ionization energy to this state determined by PES,[20] 9.82 ± 0.01 eV, is in better agreement with that of the *gauche* form, Table I.

The fact that the product ion signal is detected by one-photon MATI means that dissociation of 1-iodopropane in a high Rydberg state occurs in the ion core and the C_3H_7 moiety retains the Rydberg electron just as in the case of 2-iodopropane. Furthermore, appearance of both the parent and fragment ion signals in the MATI spectra suggests that the lifetime of the *gauche* form at the upper spin–orbit state onset is comparable to the time delay between the VUV excitation and the PFI pulse, ~40 μs. We also recorded the metastable ion decomposition spectrum for the same reaction with the double focusing mass spectrometer and could reproduce the spectral feature reported by Rosenstock and coworkers. The metastable ion peak in this case was much stronger than that for the $2\text{-}C_3H_7I^+ \rightarrow 2\text{-}C_3H_7^+ + I$ case, indicating longer lifetime. Based on this observation, we estimate that the threshold rate constant for the dissociation of 1-iodopropane ion is around 10^4-10^5 s^{-1}, which is compatible with the dissociation time span of ~40 μs mentioned above.

With the fragmentation onset very close to that of the upper spin–orbit state of the *gauche* form, 9.8332 ± 0.0017 eV, identity of the products can be determined based on the

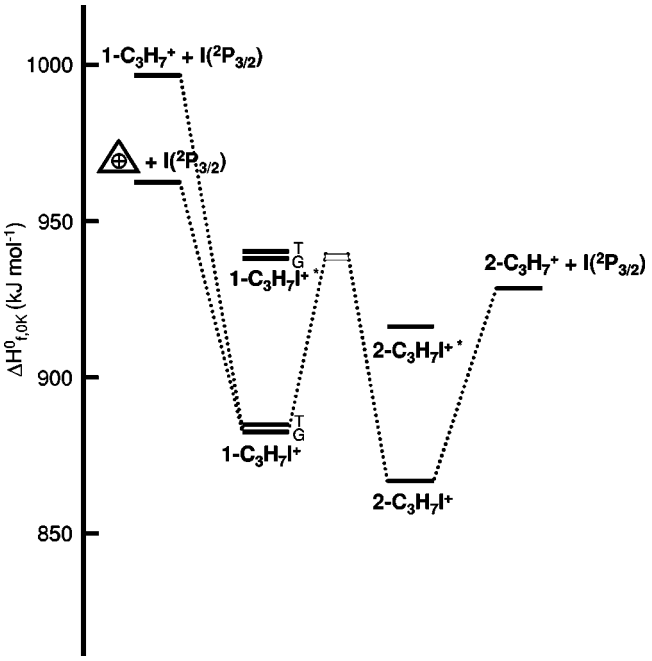

FIG. 5. Potential energy diagram for the $C_3H_7I^+$ system. * indicates the upper spin–orbit state. *G* and *T* are for *gauche* and *trans* conformers, respectively.

thermochemical data. The heats of formation at 0 K of 1-$C_3H_7I^+$, 2-$C_3H_7I^+$, and 2-$C_3H_7^+$+I($^2P_{3/2}$) have been calculated using those for the neutrals and the ionization and appearance energies obtained in this work. Protonated cyclopropane ion is another stable form of $C_3H_7^+$. 851.2 kJ mol^{-1} has been taken as its heat of formation as quoted by Baer and co-workers.[10] For the unstable form, 1-$C_3H_7^+$, 899 kJ mol^{-1} calculated by the same investigators has been adopted. Since the upper spin–orbit state of iodine atom, $^2P_{1/2}$, lies 91 kJ mol^{-1} higher in energy than $^2P_{3/2}$, and is not accessible in the present work, reactions leading to this state have not been considered. These thermochemical data are drawn as a potential energy diagram in Fig. 5. It is obvious from the figure that only 2-$C_3H_7^+$ and I($^2P_{3/2}$) can be produced in the threshold dissociation of 1-$C_3H_7I^+$.

As mentioned previously, there are three strong experimental evidences for the slow dissociation of 2-$C_3H_7I^+$ at the upper spin–orbit state onset. These are a slight shift of the breakdown diagram with the change in the source residence time in the threshold PEPICO experiment,[9] observation of strong metastable ion decomposition, and appearance of both parent and fragment ion signals after 40 μs delay in the MATI spectroscopy. Based on these, we estimated 10^4–10^5 s^{-1} as the threshold rate constant for the dissociation of 1-$C_3H_7I^+$ to 2-$C_3H_7^+$+I. In the following, we will consider some plausible mechanisms for dynamics of this reaction to account for this slow threshold rate.

In the MATI spectrum of 2-iodopropane, complex structures appeared at and above the upper spin–orbit state onset indicating strong coupling between this state and the lower state vibrational quasicontinuum. Such structures are absent in the parent and fragment ion MATI spectra of 1-iodopropane. However, this does not rule out possibility of weak coupling between these states and subsequent conversion from the upper to lower spin–orbit states. If dissociation or isomerization of 1-$C_3H_7I^+$ occurs in the lower state, the corresponding rate constant will be minimum when the reaction threshold lies at the same energy as the upper state onset. Assuming that the reaction proceeds statistically, we have calculated the minimum of the rate constant using the Rice–Ramsperger–Kassel–Marcus (RRKM) theory.[31] Since the vibrational frequencies of 1-$C_3H_7I^+$ were not available, those for the neutral in the literature were used. The minimum RRKM rate constant thus obtained is 3×10^7 s^{-1} for the *gauche* conformer. It is to be emphasized that this is the minimum for any processes, dissociation, isomerization, conformational change, etc. which may occur statistically from the ionic ground state without quantum mechanical tunneling. Considering that the observed threshold rate constant is 10^4–10^5 s^{-1}, none of the configurational changes in the lower spin–orbit state can be the rate-determining step in this case. Namely, one must assume that the conversion from the upper to lower spin–orbit state itself be rate-determining and the reaction proceed rapidly thereafter. Another possibility is that a reaction barrier exists along the reaction coordinate in the lower spin–orbit state. If the barrier is higher than the upper spin–orbit state onset and the reaction proceeds via quantum mechanical tunneling below this barrier, the slow threshold rate constant can be explained.

If the upper to lower spin–orbit state conversion is rate-determining, one does not have to assume that the fragmentation threshold be close to the upper state onset. Namely, the experimental observation can be explained even if it is lower than the upper state onset. We attempted to obtain information on the fragmentation threshold through *ab initio* calculation. This was not successful. It is to be noted, however, that the fragment ion MATI signal was not observed at all below the upper spin–orbit state onset of 1-$C_3H_7I^+$. On the other hand, the fragment ion MATI signal was observed for 2-$C_3H_7I^+$ in the upper spin–orbit state even when the parent ion MATI signal got very weak due to the poor Franck–Condon factor. Hence, it is likely that the fragmentation threshold for 1-$C_3H_7I^+$ must lie close to the upper spin–orbit state onset even if the dissociation occurs in the lower state. Also, this is in agreement with the postulation by Rosenstock and co-workers.[9] It is interesting to note that the fragmentation critical energy for 1-$C_3H_7I^+$, 0.5765 eV, is not much different from that for 2-$C_3H_7I^+$, 0.6425 eV.

It is also possible that the fragmentation of 1-$C_3H_7I^+$ proceeds on the upper spin–orbit state potential energy surface. In this case, the important experimental aspect which must be accounted for is the fact that the fragmentations of the *gauche* and *trans* forms, which differ by only 109 cm^{-1} in energy, proceed with substantially different rate constants, the former with 10^4–10^5 s^{-1} and the latter with $\sim10^6$ s^{-1} or larger. Also needed is the explanation for the fact that fragmentation proceeds on the microsecond time scale even though the fragmentation threshold is so close to the upper spin–orbit state onset. One of the plausible mechanism is that the reaction proceeds via rate-determining hydrogen transfer from C_2 to C_1 position followed by elimination of the iodine atom.

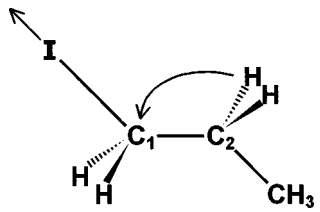

If the fragmentation threshold is a little higher than the upper spin–orbit state onset of the *gauche* conformer and the hydrogen transfer proceeds via quantum mechanical tunneling, the widely different rate constants for the *gauche* ($10^4-10^5\ s^{-1}$) and *trans* ($10^6\ s^{-1}$) conformers in their upper state origins can be explained. The hydrogen transfer in the *trans* form may be further aided by its geometrical advantage in the case when the torsional motion associated with the *gauche–trans* transformation is strongly coupled to the reaction coordinate. Considering the reaction mechanisms described so far, we set the fragmentation threshold in the energy region between the upper spin–orbit state onsets of the *gauche* and *trans* conformers, Fig. 5.

It has been generally thought that fragmentation of 1-$C_3H_7I^+$ proceeds via isomerization to the 2-$C_3H_7I^+$ structure.[9,10] For 1-$C_3H_7I^+ \rightarrow$2-$C_3H_7I^+$ isomerization, however, not only hydrogen but also heavy iodine atom must change their positions. Therefore, even if the equilibrium geometry of 2-$C_3H_7I^+$ lies along the minimum energy path from 1-$C_3H_7I^+$ to 2-$C_3H_7^+ + I$, actual dynamics may proceed via the intramolecular process described above, namely without isomerization. Calculation of the potential energy surface for this reaction and dynamics study thereon would be useful in this regard.

IV. SUMMARY AND CONCLUSION

Vacuum UV mass-analyzed threshold ionization spectroscopy has been carried out for 1- and 2-iodopropanes prepared in the supersonic jet. Molecules in the supersonic jet have minimal internal energies and the VUV laser pulse which was generated by four-wave mixing in a Kr gas cell has a spectral bandwidth of $\sim 1\ cm^{-1}$. Therefore, ionization energies to the lower and upper spin–orbit states are both accurately and precisely determined in the present work. For 2-iodopropane ion, ionization energies are $74\,005 \pm 4$ and $78\,157 \pm 14\ cm^{-1}$ for its lower and higher spin–orbit states, respectively. *Gauche* and *trans* conformers of 1-iodopropane ion are clearly resolved in the MATI spectra, giving the lower and upper state ionization energies of $74\,660 \pm 4$ and $79\,310 \pm 14\ cm^{-1}$ for the *gauche* conformer and $74\,782 \pm 4$ and $79\,419 \pm 14\ cm^{-1}$ for the *trans* conformer, respectively. Since *gauche* and *trans* conformers can be hardly separated by conventional experimental methods, separation of these conformers achieved in this work is quite meaningful and may have practical applicability. In particular, capability to generate each conformeric ion beam selectively opens up a new way to study the geometrical effect on ion spectroscopy and dynamics.

Ion core dissociation dynamics are also revealed in MATI spectra probing both parent and fragment ions. The threshold energies for ion fragmentation are determined from the excitation energies where the MATI signals due to fragment ions start to appear. The fragmentation threshold for 2-iodopropane ion is determined to be $79\,188 \pm 29\ cm^{-1}$. The dissociation rate of $10^5-10^6\ s^{-1}$ at the threshold energy is estimated from the metastable ion decomposition spectrum obtained with a double focusing mass spectrometer. The same method has been used to estimate the dissociation rate constant of 1-iodopropane ion in the threshold region, which is $10^4-10^5\ s^{-1}$. Especially, the MATI spectra of parent and fragment ions of 1-iodopropane observed at the upper spin–orbit state of the *gauche* form confirm this estimation of the rate constant. The slow rate constant for the dissociation of 1-iodopropane ion indicates that a reaction barrier may exist along the reaction coordinate. That is, at the upper-state origin of the *gauche* conformer, the reaction is likely to proceed via the quantum-mechanical tunneling through this barrier. Meanwhile, the excitation energy corresponding to the upper-state of the *trans* form is at or just above the reaction barrier, and the dissociation takes place with a relatively faster rate. Dissociation of 1-iodopropane ion does not occur with a simple bond-rupture mechanism in the threshold region. Rather, the reaction coordinate should involve the transfer of the H-atom and possibly the torsional motion associated with the *gauche–trans* transformation. Detailed theoretical study on the configurational change along the minimum energy path and on the actual dynamics would be useful to unravel the nature of this reaction.

The present work provides the accurate potential energy diagram for the dissociation of iodopropane ions. Overall, the values associated with photoionization and ion fragmentation reported in this work are in reasonable agreement with those previously determined by PES, PEPICO, or PFI-PEPICO spectroscopic methods, even though differences beyond the error limits have been observed for some values. Since the present data are thought to be more accurate, associated thermodynamic quantities have been refined. These are the heat of formation at 0 K of 2-$C_3H_7^+$, $821.7 \pm 3.8\ kJ\,mol^{-1}$ and the proton affinity at 0 K of C_3H_6, $741.6 \pm 3.9\ kJ\,mol^{-1}$.

ACKNOWLEDGMENTS

Authors thank C. H. Kwon for the measurement of metastable ion decomposition spectra. This work was supported financially by CRI, the Ministry of Science and Technology, Republic of Korea. S. T. Park thanks the Ministry of Education, Republic of Korea, for the financial support through the Brain Korea 21 program.

[1] K. Müller-Dethlefs, M. Sander, and E. W. Schlag, Chem. Phys. Lett. **112**, 291 (1984).
[2] I. Fischer, R. Lindner, and K. Müller-Dethlefs, J. Chem. Soc., Faraday Trans. **90**, 2425 (1994).
[3] K. Müller-Dethlefs and E. W. Schlag, Annu. Rev. Phys. Chem. **42**, 109 (1991).
[4] E. W. Schlag, *ZEKE Spectroscopy* (Cambridge University Press, Cambridge, 1998).
[5] J. W. Hepburn, Chem. Soc. Rev. **25**, 281 (1996).
[6] L. Zhu and P. Johnson, J. Chem. Phys. **94**, 5769 (1991).
[7] H. Krause and H. J. Neusser, J. Chem. Phys. **97**, 5923 (1992).
[8] (a) J. C. Traeger, Int. J. Mass Spectrom. Ion Phys. **32**, 309 (1980); (b) J. C. Traeger and R. G. McLoughlin, J. Am. Chem. Soc. **103**, 3647 (1981).

[9] H. M. Rosenstock, R. Buff, M. A. A. Ferreira, S. G. Lias, A. C. Parr, R. L. Stockbauer, and J. L. Holmes, J. Am. Chem. Soc. **104**, 2337 (1982).
[10] W. A. Brand and T. Baer, Chem. Phys. **76**, 111 (1983).
[11] T. Baer, Y. Song, C. Y. Ng, J. Liu, and W. Chen, J. Phys. Chem. A **104**, 1959 (2000).
[12] R. Hilbig, A. Lago, and R. Wallenstein, J. Opt. Soc. Am. B **4**, 1753 (1983).
[13] J. P. Marangos, N. Shen, H. Ma, M. H. R. Hutchinson, and J. P. Connerade, J. Opt. Soc. Am. B **7**, 1254 (1990).
[14] S. A. Meyer and G. W. Faris, Opt. Lett. **23**, 204 (1998).
[15] E. Nir, H. E. Hunziker, and M. S. De Vries, Anal. Chem. **71**, 1674 (1999).
[16] R. Lindner, H. Dietrich, and K. Müller-Dethlefs, Chem. Phys. Lett. **228**, 417 (1994).
[17] (a) A. Held, U. Aigner, L. Y. Baranov, H. L. Selzle, and E. W. Schlag, Chem. Phys. Lett. **299**, 110 (1999); (b) A. Held, L. Y. Baranov, H. L. Selzle, and E. W. Schlag, *ibid.* **291**, 318 (1998); (c) A. Held, H. L. Selzle, and E. W. Schlag, J. Phys. Chem. **100**, 15314 (1996).
[18] M. S. Kim, C. H. Kwon, and J. C. Choe, J. Chem. Phys. **113**, 9532 (2000).
[19] N. Knoblauch, A. Strobel, I. Fischer, and V. E. Bondybey, J. Chem. Phys. **103**, 5417 (1995).
[20] K. Kimura, S. Katsumata, Y. Achiba, T. Yamazaki, and S. Iwata, *Handbook of HeI Photoelectron Spectra of Fundamental Organic Molecules* (Japan Scientific Societies, Tokyo, 1981).
[21] (a) A. D. Baker, D. Betteridge, N. R. Kemp, and R. E. Kirby, Anal. Chem. **43**, 375 (1971); (b) K. Kimura, S. Katsumata, Y. Achiba, H. Matsumoto, and S. Nagakura, Bull. Chem. Soc. Jpn. **46**, 373 (1973); (c) R. A. A. Boschi and D. R. Salahub, Can. J. Chem. **52**, 1217 (1974).
[22] GAUSSIAN 98, Revision A.6, M. J. Frisch, G. W. Trucks, H. B. Schlegel *et al.* (Gaussian, Inc., Pittsburgh, PA, 1998).
[23] (a) H. J. Neusser and H. Krause, Chem. Rev. **94**, 1829 (1994); (b) H. Krause and H. J. Neusser, J. Chem. Phys. **99**, 6278 (1993).
[24] A. Mank, T. Nguyen, J. D. D. Martin, and J. W. Hepburn, Phys. Rev. A **51**, R1 (1995).
[25] (a) B. J. Smith and L. Radom, J. Phys. Chem. **99**, 6468 (1995); (b) Chem. Phys. Lett. **231**, 345 (1994); (c) J. Am. Chem. Soc. **115**, 4885 (1993).
[26] (a) W. E. Steinmetz, F. Hickernell, and I. K. Mun, J. Mol. Spectrosc. **68**, 173 (1977); (b) Y. Niide, I. Ohkoshi, and M. Takano, *ibid.* **122**, 113 (1987); (c) M. Fujitake and M. Hayashi, *ibid.* **127**, 112 (1988).
[27] (a) D. L. Philips, B. A. Lawrence, and J. J. Valentini, J. Phys. Chem. **95**, 7570 (1991); (b) X. Zheng and D. L. Phillips, J. Chem. Phys. **108**, 5772 (1998); (c) Mol. Phys. **96**, 1051 (1999).
[28] K. Hagen, R. Stølevik, and P. C. Sæbo, J. Mol. Struct. **346**, 75 (1995).
[29] J. D. Pitts, J. L. Knee, and S. Wategaonkar, J. Chem. Phys. **110**, 3378 (1999).
[30] F. G. Godwin, C. Paterson, and P. A. Gorry, Mol. Phys. **61**, 827 (1987).
[31] K. A. Holbrook, M. J. Pilling, and S. H. Robertson, *Unimolecular Reactions*, 2nd ed. (Wiley, New York, 1996).
[32] J. B. Pedley, R. D. Naylor, and S. P. Kirby, *Thermochemical Data of Organic Compounds* (Chapman and Hall, London, 1986).
[33] (a) D. D. Wagman, W. H. E. Evans, V. B. Parker, R. H. Schum, I. Halow, S. M. Mailey, K. L. Churney, and R. L. Nuttall, The NBS Tables of Chemical Thermodynamic Properties, in J. Phys. Chem. Ref. Data Suppl. **11**, 2 (1982); (b) J. D. Cox, D. D. Wagman, and V. A. Medvedev, *CODATA Key Values for Thermodynamics* (Hemisphere, New York, 1989).
[34] S. G. Lias, J. E. Bartmess, J. F. Liebman, J. L. Holmes, R. D. Levin, and W. G. Mallard, Gas-Phase Ion and Neutral Thermochemistry, J. Phys. Chem. Ref. Data Suppl. **17**, 1 (1988).
[35] J. E. Szulejko and T. B. McMahon, J. Am. Chem. Soc. **115**, 7839 (1993).
[36] W. Koch, B. Liu, and P. v. R. Schleyer, J. Am. Chem. Soc. **111**, 3479 (1989).